https://doi.org/10.48048/tis.2023.6558

Theoretical Investigations on the Interactions of Urea with Hydroxyl and Non-Hydroxyl Hydroxyapatite Surface

Nur Adlin Sofiya Mohammad Fuad, Lee Sin Ang*, Nur Najwa Alyani Mohd Nabil and Norlin Shuhaime

Faculty of Applied Sciences, Universiti Teknologi MARA Perlis Branch Arau Campus, Perlis 02600, Malaysia

(*Corresponding author's e-mail: anglee631@uitm.edu.my)

Received: 31 December 2022, Revised: 19 February 2023, Accepted: 21 February 2023, Published: 16 March 2023

Abstract

We performed an investigation on urea interacting with hydroxyapatite (HA). The oxygen atoms on HA are either left alone or added with hydrogen to create hydroxyl to resemble the HA surface. Using B3LYP and 3 different basis sets, it was found that urea was able to interact positively with either hydroxyl or non-hydroxyl surface of HA. The Gaussian 09 and Multiwfn software were employed to conduct the calculations. The most favorable interaction has interaction energy of –1.36 eV, which was obtained with the 2 largest basis sets considered, on the pure hydroxyl surface. From the topology analysis on electron density and the non-covalent interaction analysis, it was found that the main attractions between urea and HA were due to the carbonyl oxygen and hydrogen of urea, and hydrogen, oxygen, and calcium on the HA surface. The bond length of newly bonded atoms ranges from 1.62 to 5.18 Å, whereas the energy gap has range between 0.46 to 1.14 eV. All the analysis performed in this study agreed with the results obtained in the formation of favorable interactions and complement previous experimental results that HA can bond with urea molecule.

Keywords: Density functional theory, Electrostatic potential surface, Frontier molecular orbital, Hydroxyapatite, Hydrogenation, Interaction energy, Non-covalent interaction, Topology analysis, Urea

Introduction

Phosphorus and nitrogen are two of the essential macronutrients that necessary for plants growth [1,2]. The most common source of nitrogen is urea, which are used as synthetic fertilizer. Phosphorus is typically provided *via* hydroxyapatite (HA) nanoparticles, which have excellent biocompatibility and large surface area that may help in the binding of a large amount of urea [3]. Furthermore, since nanoparticles can easily be diffused or migrated into soil and reach the plants through the transpiration process, the potential use of HA nanoparticles as a source of phosphorus fertilizer has been proven in enhancing phosphorus efficiency [4,5]. However, due to several factors, these 2 macronutrients are easily washed away. For example, environmental factors cause the loss of nutrients under conditions of high valorization and humidity, even before they reach the plants [1,6-10]. For ecological systems, excessive use of nitrate and phosphate fertilizers can cause eutrophication effect to the aquatic ecosystem. For human health, too much exposure, ingestion of nitrate and nitrite can cause acute toxic response that prevents the transportation of oxygen to the blood and contributes to the development of digestive tract [11-15]. Economically, using too much fertilizers can results in financial losses of farmers by having to buy more fertilizers for their crops and treating disease that caused by excessive exposure to hazardous chemicals from the fertilizers [11-14].

To address these problems, slow-release fertilizers were developed to assist the delivery of the nutrients to the crops in slow manner, hence enhancing macronutrients consumption [9]. This slow-release method has been proven to reduce the suspension [16], and the volatilization rate of urea while preventing phosphate immobilization in soil [1]. The efficiency of slow-release fertilizer by using urea-HA nanoparticle have been verified experimentally. For example, even with a 50 % reduction in urea concentration, significant increment in the tea yields have been achieved [17]. In another research, improved rice crops have been obtained while maintaining the quantity yields [3].

Experimental works have been previously performed on the interactions between components of the urea-HA nanohybrids. In the work focused on the delivery of nutrients to rice crops by slow-release fertilizer of urea-HA nanohybrids, X-Ray photoelectron spectroscopy (XPS) showed the formation of a new connection between urea and HA through the nitrogen atom of urea. On HA, the binding energy of phosphorus 2p is found to increase to the higher level, implying that the electron density around phosphorus has been influenced and that a new hydrogen bonding between phosphate group in HA and urea may have formed. Binding energy in calcium ions has also increased, probably due to the chemical environment that has changed when urea was introduced to the HA [3]. In another study, Fourier transform infrared spectroscopy (FTIR) analysis on urea-modified HA encapsulated into soft-wood cavities [2], shows the presence of hydrogen bonding between hydroxyl group in HA with N-H group in urea. Comparison made between pure urea and urea-HA indicates changes in electron density that may have been influenced by new hydrogen bonding of N-H in HA [2]. Besides, the N-H stretching showed marked shift in urea-HA and the shifted energy in Ca 2p core level for HA suggested that the chemical environment near calcium ions is affected by the presence of urea on HA surface. Energy core level of phosphorus 2p in HA also changed to higher binding energy after binding to urea that implies a new interaction happened between oxygen atom in phosphate group on HA and hydrogen atom of amide in urea [18]. In addition, many previous studies were using HA as binding site for other molecules to attach. For instance, the hexagonal structure of HA binds with lysine, water and collagen [19-21]. On HA surfaces, calcium atoms, hydrogen and oxygen atoms are responsible for creating a new bonding with foreign molecules. These atoms have been noted in creating the HA cluster and placing the urea molecule. The results indicate that HA is flexible in binding molecules into its surface.

Urea-HA is to be used as a slow-release fertilizer [2,3], in which the application of the said compound has also been performed, in the field trial in rice paddy [3]. With the success in the previous experimental study of urea-HA [1-4,17,18,22-26], we set out to investigate, theoretically, the behavior of the urea attached to HA. This article focused on the interaction between urea-HA in identifying the strength of this combination, the functional groups involved in IR spectra, the reactive side on HA surfaces and the interactions involved in the bonding.

Materials and methods

Computational details

In this study, DFT based calculations, in the form of B3LYP hybrid functional and 6-31G(d,p) basis set has been implemented by using the Gaussian 09 suite of program [27]. B3LYP/6-31G(d,p) has been used in a number of previous studies, including detecting interaction between ions in gas phase of ionic liquid and on large set of organic molecules [28]. Single point calculations were also performed at the optimized geometries with higher basis sets, namely DEF2-TZVP and 6-311++G(2df,2pd). These 2 basis sets acted as a comparison to the values obtained at level 6-31G(d,p).

Monoclinic crystal structure of HA as reported by Elliot *et al.* [29], was referred and used to create the structure of HA for the deposition of urea. The obtained structure is as shown in **Figure 1**. Three different clusters were obtained by truncating the crystal structure of HA as to model 3 different surface terminations: *Viz.,* the first cluster with present of hydroxyl group (labeled as HA1), the second cluster structure without the hydroxyl group (HA2) and the third cluster structure (HA3) that combines the first and second clusters. These 3 types of HA structure are considered as there is no experimental evidence that confirmed the existence of specific arrangement. Hydrogenation method [30], was used to create the hydroxyl groups. This type of termination of hydrogen has been used many past studies. For example, oxygen atoms in kaolinite cluster, montrillonite clay and molybdenum trioxide were set as boundary and saturated it with hydrogen atoms [31-33]. According to Bystrov [34], and Bystrov *et al.* [30], if the oxygen atoms or any hydroxyl group molecules are attached on HA surface, a negative charge will occurs and the electrostatic field around the HA surface will be more negative. This will eventually help in enhancing the attachment of other molecules on it. **Figure 2** shows the initial structure of HA1, HA2 and HA3 before and after been truncated with hydrogen, prior to the addition of urea molecule.

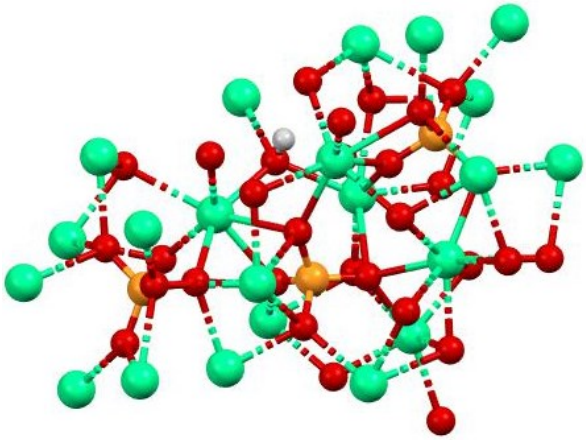

Figure 1 Structure of monoclinic HA as viewed by using mercury software [35]. The red spheres are oxygen, the orange spheres are phosphorus, and green spheres are calcium.

A urea molecule was placed on HA surfaces based on chemical intuition of electrostatic potential (ESP). Urea atom was placed on the HA surface which shown electrophilic characters. **Figure 3** shows the initial placement of urea on HA1, HA2 and HA3 surfaces.

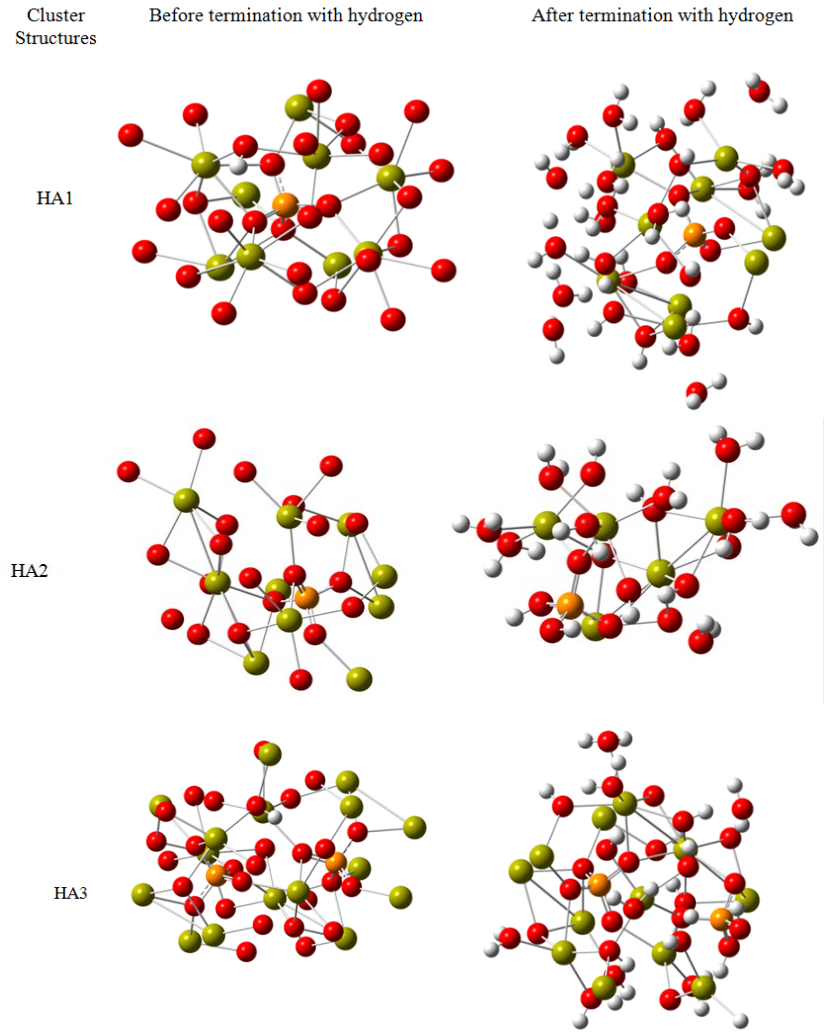

Figure 2 The initial structure of HA1, HA2 and HA3 before and after termination with hydrogen. The green, white and red ball-and-stick corresponds to calcium, hydrogen and oxygen.

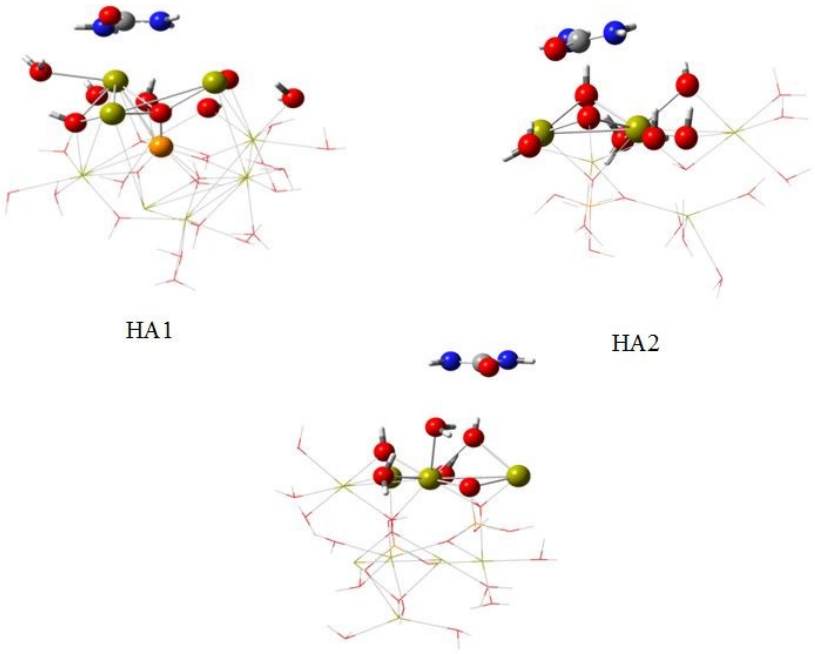

Figure 3 The initial placement of urea on HA1, HA2 and HA3 surfaces. The blue represents nitrogen atom, the red represents oxygen atom, the green represents calcium atom and grey represent carbon atom. The atoms distant from urea, represented with wireframe scheme, are fixed, while the ball-and-stick atoms are relaxed. For clarity, the hydrogen atoms on the surface of HA are represented in tube form.

$$E_{int} = E_{HA+Urea} - (E_{HA} + E_{Urea}) \quad (1)$$

Eq. (1) was used to determine the relative stability of urea-HA. This equation has been used in many past studies in finding and calculating the interaction energy, adsorption energy or binding energy involving 2 components related to HA [19-21,36]. E_{int} is the interaction energy between urea-HA, $E_{HA+Urea}$ is the total energy of urea-HA after geometry optimization, E_{HA} is the energy of HA and E_{Urea} is the total energy of urea. All the energies values are expressed in eV. According to Eq. (1), the more negative the interaction energy (E_{int}), the stronger the bonding between urea and HA.

Multiwfn program [37], is used to perform the electron density topology analysis for newly formed bond, non-covalent interaction (NCI) and electron localization function (ELF). The topology analysis is performed to find new bond form by searching the critical points (CPs). Meanwhile, NCI is usually applied in determining the type of weak interaction based on reduced density gradient (RDG) at the low densities [38]. RDG is color-filled that has been mapped on isosurfaces of all combinations with different color scale. **Figure 4** shows the RDG isosurface of color scale with the type of bonding involved. According to the color scale, the blue indicates a greater attractive interaction, green or light brown indicates a low electron density or van der Waals interaction, and red indicates a steric effect interaction.

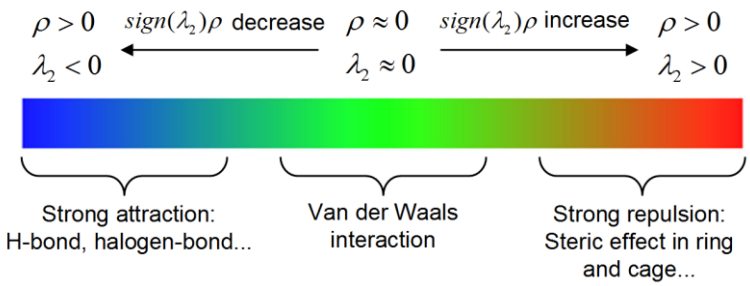

Figure 4 The color scale of reduced density gradient isosurface (RDG), according to Lu and Chen [37].

Results and discussion

Geometries of the combinations

ESP was used for the initial placements of the urea molecule on the clusters. **Figure 5** shows the ESP surface that was mapped on HA1, HA2 and HA3 clusters, before addition of urea. On the ESP surfaces of HA structures, the minimum points $V_{s,min}$ and maximum points $V_{s,max}$ have been identified. The $V_{s,min}$ and $V_{s,max}$ were denoted by the red and blue regions, respectively. The minima points in HA1, HA2 and HA3 were located near to the hydrogen atoms that are attached to the oxygen atoms. These surfaces have a lot of electrons and are vulnerable to the electrophilic attack. The maxima points were located near oxygen and calcium atoms. These surfaces are referred to as electron deficient regions, and they are vulnerable to nucleophile attack. Based on these ESP results of HA clusters, urea molecule were placed horizontally on negative or slightly negative charge region.

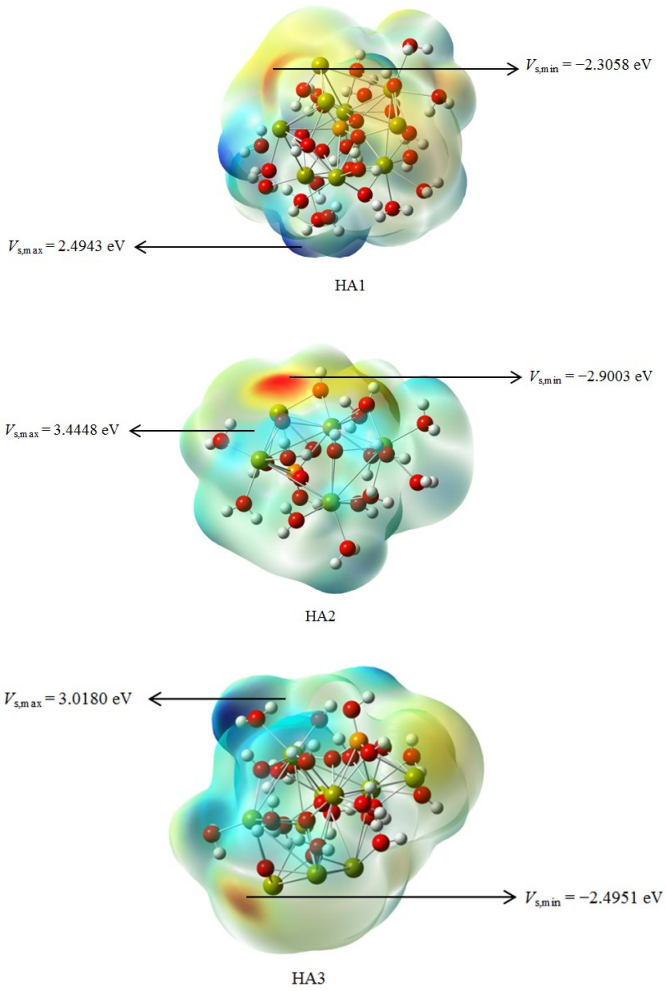

Figure 5 The ESP surface mapped on HA1, HA2 and HA3. Oxygen atoms are red, calcium atoms are green and hydrogen atoms are white in ball-and-stick schemes.

Figure 6 shows the final arrangement of combination urea with HA1, HA2 and HA3. The final position of urea-HA1, urea-HA2 and urea-HA3 were changed to vertical positions from the horizontal positions. These urea molecules were initially placed on the yellow or red region on HA surfaces, however the urea molecules in HA1, HA2 and HA3 were moved to blue region on HA surface accordingly to the chemical behavior of the atoms.

Based on the ESP obtained, the hydrogen atoms in urea acted as electrophilic sites while oxygen and nitrogen atoms acted as nucleophile sites. Nucleophile atoms of urea were attracted to the electrophilic sites on HA, which was the positive site of blue color region based on the color scale of ESP, and the electrophilic sites of urea were attracted to the nucleophile sites of red color region on HA surfaces.

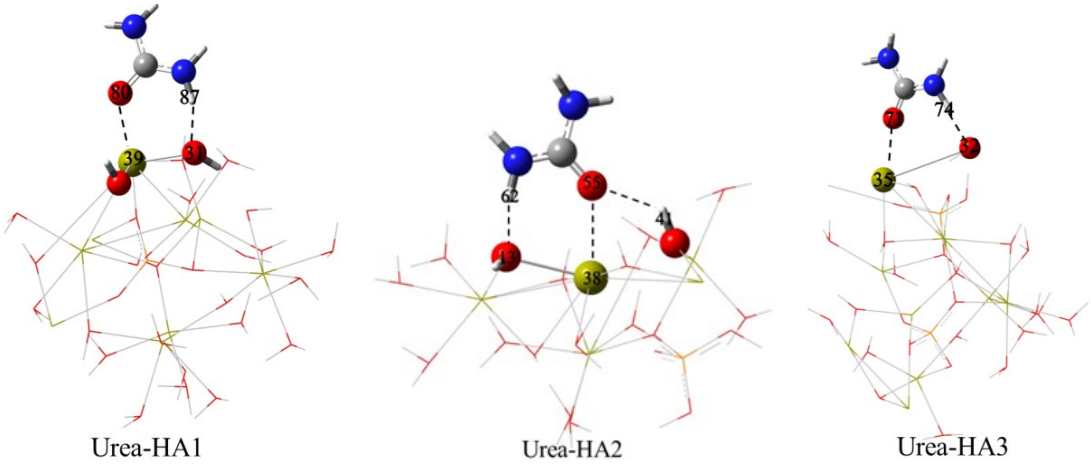

Figure 6 The final arrangements of combinations of urea with HA1, HA2 and HA3. The red, green, blue and grey ball-and-stick schemes represent oxygen, calcium, nitrogen and carbon atoms respectively. The tube type present hydrogen atoms. The distant atoms are presented in wireframe form.

Table 1 shows the bond lengths of new bond formed before and after optimization for urea combinations with HA1, HA2 and HA3. The newly bonded atoms in **Table 1** are labeled and shown **Figure 6**. All the combinations had formed new chemical bonds of oxygen-calcium and hydrogen-oxygen. Their bond lengths become shorter after optimized, which indicates there are strong attraction and interaction happened between urea and HA. The interaction of hydrogen atom in urea or HA with oxygen atom in urea or HA had previously been studied experimentally, where revealed N-H stretching has shifted to a lower wavenumber in urea-HA spectrum and carbonyl group wavenumber also has shifted to low value which may been affected by the new bonding formed [2]. In addition, XPS analysis shows that the chemical environmental of calcium atoms had changed after urea molecule was introduced to the HA surface [3].

Table 1 Bond length of new bond formed for urea-HA1, urea-HA2 and urea-HA3 before and after optimization.

Combinations	Interested atom pairs	Bond length (Å)	
		Before optimization	After optimization
Urea-HA1	O80…Ca39	2.9102	2.3280
	H87…O31	1.8840	1.7445
Urea-HA2	O55…Ca8	4.5399	2.5715
	O55…H41	3.0197	2.0647
	H62…O13	4.2578	1.6176
Urea-HA3	O71…Ca35	5.1764	2.3579
	H74…O32	4.2500	1.7600

Frontier molecular orbitals

From the values tabulated in **Table 2**, it can be seen that HA2 has larger HOMO-LUMO energy gap, compared to the other 2 structures, where HA1 and HA3 have lesser than half the HOMO-LUMO energy gap of HA2. Larger energy gap is related to higher kinetic stability [39,40], hence, the non-hydrogen terminated surface of HA2 has higher kinetic stability than HA1 and HA3. On the other hand, HA3 has higher stability than HA1, as HA3 is the combination of bare and hydroxyl surfaces.

Table 2 The HOMO, LUMO and calculated energy gap of HA1, HA2 and HA3 energies. All energy values are in eV.

Structures	E_{HOMO} (eV)	E_{LUMO} (eV)	E_{gap} (eV)
HA1	−2.1902	−1.7317	0.4585
HA2	−2.6147	−1.4708	1.1439
HA3	−1.8626	−2.3445	0.4819

The HOMO and LUMO orbitals for HA1, HA2 and HA3 clusters are shown in **Figures 7**. As shown in the figure, the HOMO and LUMO lobes were found near the calcium atoms and hydroxyl molecules. The orbitals of the HOMO and LUMO lobes of HA cluster structures also coincide with the previous studies, in which both the orbitals were delocalized on calcium-oxygen molecules [41].

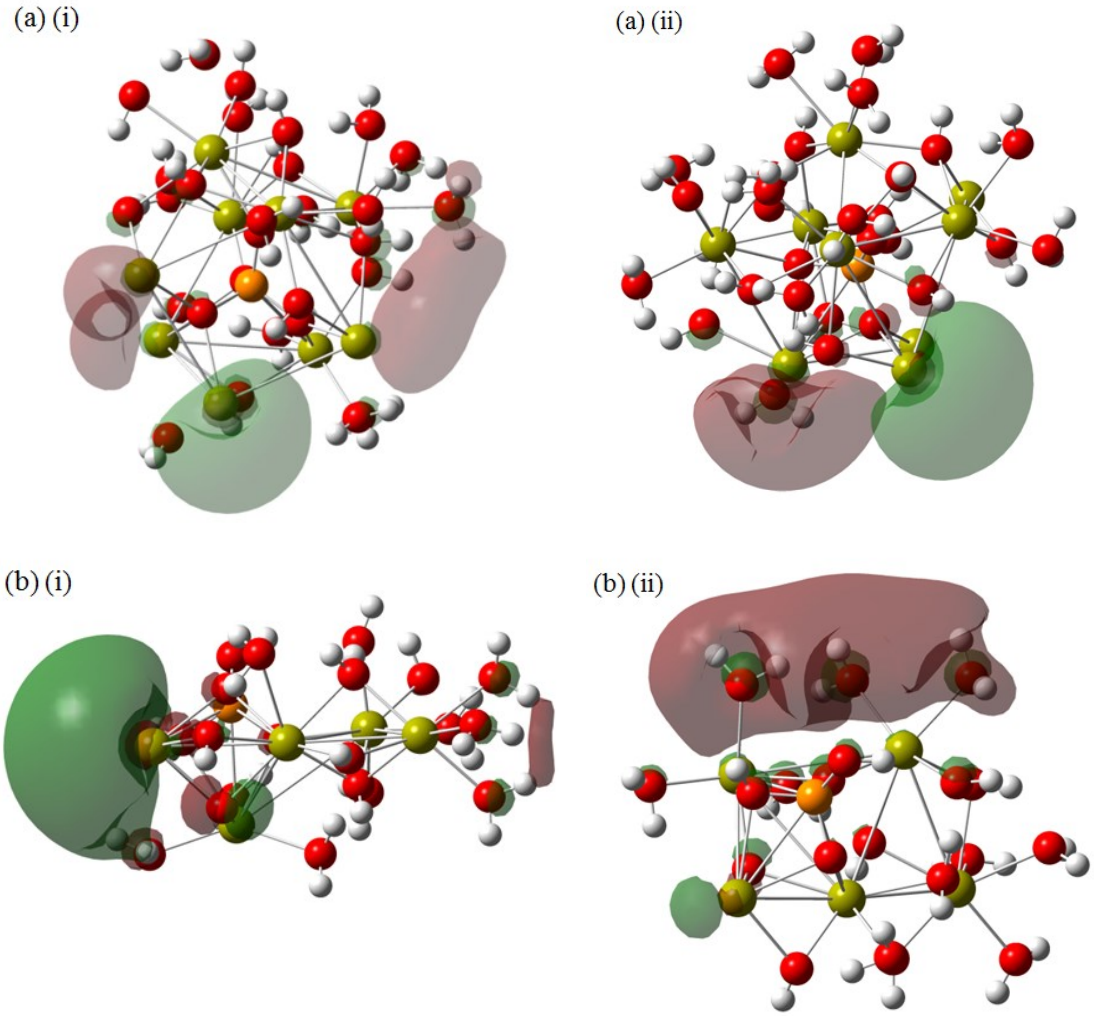

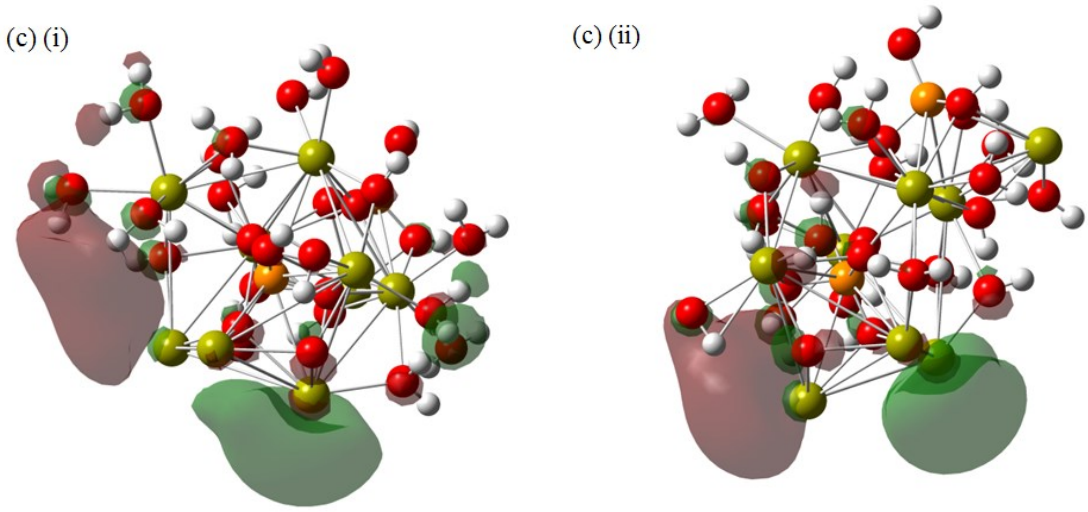

Figure 7 (i) HOMO and (ii) LUMO orbitals of (a) HA1, (b) HA2, and (c) HA3.

Topology analysis on electron density

Figure 8 shows the topology bond path for all combinations of urea-HA1, urea-HA2 and urea-HA3, respectively. The new bond path between oxygen and calcium is overlapped with the green bond, which are stronger connected pair than those without. The orange spheres correspond to bond critical points (3,-1), while yellow spheres correspond to ring critical points (3,+1).

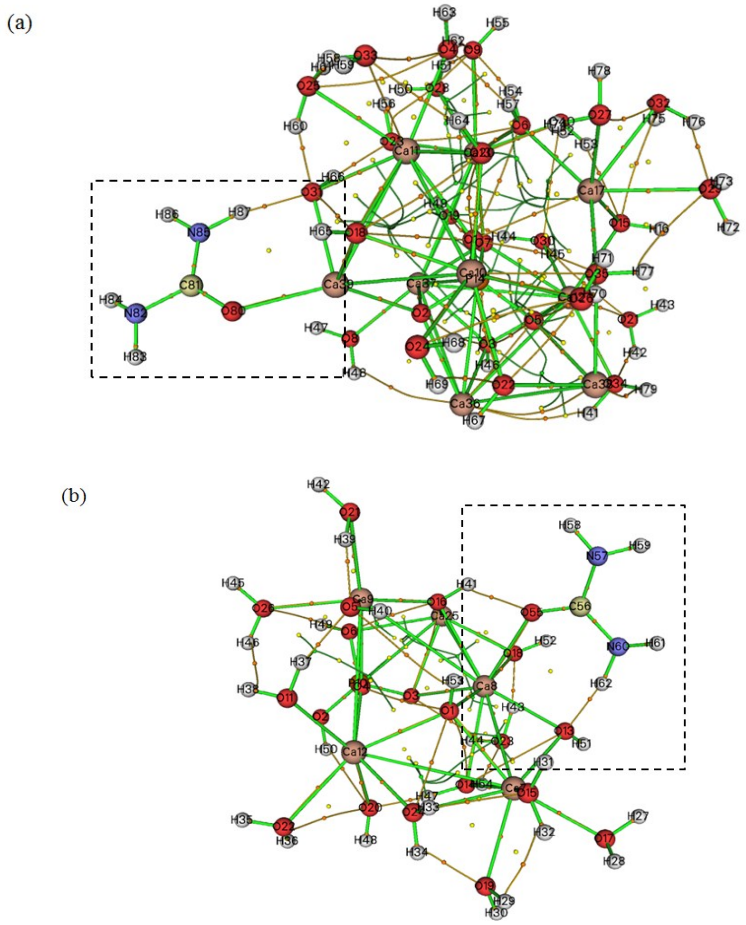

(c)

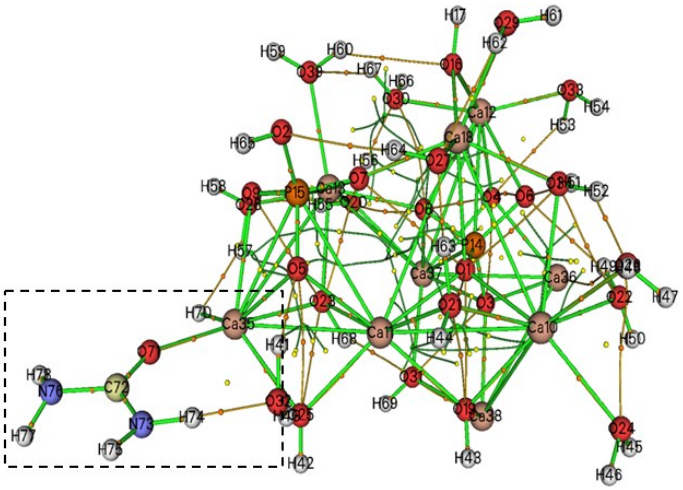

Figure 8 (a) The topology bond path of combination urea-HA1, (b) urea-HA2, and (c) urea-HA3, showing the newly formed bond paths between urea and HA. The new bond path between oxygen and calcium is overlapped with the green bond, which are stronger connected pair than those without. The regions of interest are highlighted in the solid-line boxes.

Interaction energies

Table 3 shows the interaction energies of urea-HA combinations. The strength of order for 6-31G(d,p) is, in increasing order, urea-HA1 > urea-HA2 > urea-HA3, while the trend for DEF2-TZVP and 6-311++G(2df,2pd) is urea-HA2 > urea-HA3 > urea > HA1. The trend in larger basis sets agrees with the results from E_{gap}, as HA1 has lower kinetic stability, hence higher tendency to interact with the molecules, in this case, adsorption of urea. As the geometries were optimized at 6-31G(d,p), and energy-related evaluations are using triple-zeta basis sets, the observation points to the use of triple-zeta basis sets to produce reliable results in the interaction energies. The observation agrees with the work from Nabil *et al.* [42].

Table 3 The calculated interaction energies of urea-HA1, urea-HA2 and urea-HA3 after optimization at level 6-31G(d,p), DEF2-TZVP and 6-311G++(2df,2pd).

Structures	Interaction energies (eV)		
	6-31G(d,p)	DEF2-TZVP	6-311++G(2df,2pd)
Urea-HA1	−1.5915	−1.3586	−1.3642
Urea-HA2	−1.6413	−0.9914	−1.2569
Urea-HA3	−1.6897	−1.3350	−1.3202

Non-covalent interaction (NCI)

Figure 9 shows the NCI isosurface for urea-HA1, urea-HA2 and urea-HA3. For urea-HA1 and urea-HA3, blue slab discs exist between oxygen-calcium and hydrogen-oxygen interaction. These blue isosurface slabs indicated strong attraction had occurred between the atoms in urea and HA. For urea-HA2, the same oxygen atom in urea had interacted with calcium and hydrogen atoms, but with light blue and mix blue greenish slabs between them. This observation agrees with the strength of the interaction energies (of larger basis sets), in which urea absorbed on HA1 and HA3 have higher strength, compared to on HA2, and the bond critical points in the topology analysis.

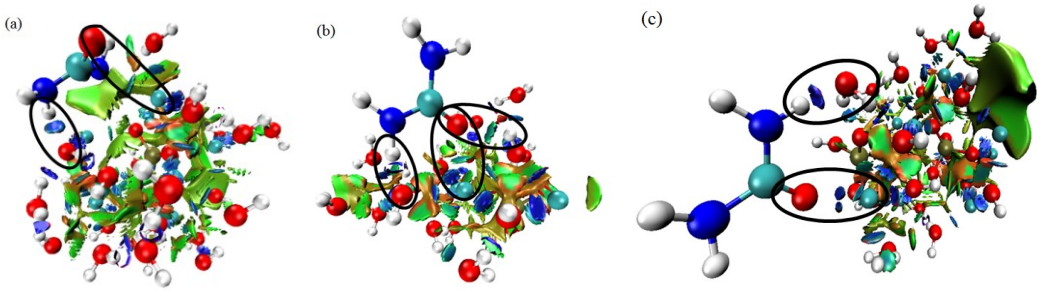

Figure 9 The NCI isosurface formed between urea and (a) HA1, (b) HA2, and (c) HA3. Oxygen is represented by red spheres; hydrogen white; nitrogen blue; calcium turquoise.

Conclusions

In this work, the urea-HA interactions are elucidated. Three different surfaces of HA are modeled: With and without hydroxyl groups (HA1, HA2), and a mixture of them (HA3). Urea molecules were positioned horizontally on negative or slightly negative charge based on the ESP results of HA. It was found that, urea is able to get adsorbed on the surfaces of these models, through the carbonyl oxygen and hydrogen of urea, and hydrogen, oxygen, and calcium on the HA surface. They have shorter bond length values after optimization compared to before. HA is found to be the most kinetically stable from the HOMO-LUMO gap, the results from this work agree with the observation in the experimental that urea is able to combine on the surface of HA, where hydroxyl termination have higher tendency to interact with urea. The analysis on the interaction indicated that the surface with hydroxyl has the highest strength. As for urea-HA1 has the highest interaction energy, at –1.36 eV for basis sets of 6-311++G(2df,2pd) and DEF2-TZVP. The urea-HA has been previously reported to have been successfully synthesized by incorporating urea molecules into HA matrix [3]. Thus, this report is considered as providing evidence from a theoretical point of view.

Acknowledgements

This study is supported by the Minister of Higher Education Malaysia in financing support through Fundamental Research Grant Scheme (FRGS, project code 600-IRMI/FRGS 5/3 (115/2019)).

References

[1] AS Giroto, GGF Guimarães, M Foschini and C Ribeiro. Role of slow-release nanocomposite fertilizers on nitrogen and phosphate availability in soil. *Sci. Rep.* 2017; **7**, 46032.

[2] N Kottegoda, I Munaweera, N Madusanka and V Karunaratne. A green slow-release fertilizer composition based on urea-modified hydroxyapatite nanoparticles encapsulated wood. *Curr. Sci.* 2011; **101**, 73-8.

[3] N Kottegoda, C Sandaruwan, G Priyadarshana, A Siriwardhana, UA Rathnayake, DM Berugoda Arachchige, AR Kumarasinghe, D Dahanayake, V Karunaratne and GAJ Amaratunga. Urea-hydroxyapatite nanohybrids for slow release of nitrogen. *ACS Nano* 2017; **11**, 1214-21.

[4] A Giroto, S Fidélis and C Ribeiro. Controlled release from hydroxyapatite nanoparticles incorporated into biodegradable, soluble host matrixes. *RSC Adv.* 2015; **5**, 104179-86.

[5] D Montalvo, MJ McLaughlin and F Degryse. Efficacy of hydroxyapatite nanoparticles as phosphorus fertilizer in andisols and oxisols. *Soil Sci. Soc. Am. J.* 2015; **79**, 551-8.

[6] ARL Cabezas, PCO Trivelin, JA Bendassolli, DGD Santana and GJ Gascho. Calibration of a semi-open static collector for determination of ammonia volatilization from nitrogen fertilizers. *Comm. Soil Sci. Plant Anal.* 1999; **30**, 389-406.

[7] L Guo, D Luo, C Li and M FitzGibbon. Preparation and properties of a slow-release membrane-encapsulated urea fertilizer with superabsorbent and moisture preservation. *Ind. Eng. Chem. Res.* 2005; **44**, 4206-11.

[8] A Jarosiewicz and M Tomaszewska. Controlled-release NPK fertilizer encapsulated by polymeric membranes. *J. Agr. Food Chem.* 2003; **51**, 413-7.

[9] L Wu and M Liu. Preparation and properties of chitosan-coated NPK compound fertilizer with controlled-release and water-retention. *Carbohydr. Polym.* 2008; **72**, 240-7.

[10] D Castro-Enríquez, F Rodríguez-Félix, B Ramírez-Wong, P Torres-Chávez, M Castillo-Ortega, D Rodríguez-Félix, L Armenta-Villegas and A Ledesma-Osuna. Preparation, characterization and release of urea from wheat gluten electrospun membranes. *Materials* 2012; **5**, 2903-16.
[11] JA Camargo and Á Alonso. Ecological and toxicological effects of inorganic nitrogen pollution in aquatic ecosystems: a global assessment. *Environ. Int.* 2006; **32**, 831-49.
[12] DC Bouchard, MK Williams and RY Surampalli. Nitrate contamination of groundwater: sources and potential health effects. *J. Am. Water Works Assoc.* 1992; **84**, 85-90.
[13] D Majumdar and N Gupta. Nitrate pollution of groundwater and associated human health disorders. *Indian J. Environ. Health* 2000; **42**, 28-39.
[14] A Shaviv. Advances in controlled-release fertilizers. *Adv. Agron.* 2001; **71**, 1-49.
[15] CG Ramos, X Querol, AC Dalmora, KCDJ Pires, IAH Schneider, LFS Oliveira and RM Kautzmann. Evaluation of the potential of volcanic rock waste from southern Brazil as a natural soil fertilizer. *J. Cleaner Prod.* 2017; **142**, 2700-6.
[16] KRM Ibrahim, FE Babadi and R Yunus. Comparative performance of different urea coating materials for slow release. *Particuology* 2014; **17**, 165-72.
[17] S Raguraj, WMS Wijayathunga, GP Gunaratne, RKA Amali, G Priyadarshana, C Sandaruwan, V Karunaratne, LSK Hettiarachchi and N Kottegoda. Urea-hydroxyapatite nanohybrid as an efficient nutrient source in Camellia sinensis (L.) Kuntze (tea). *J. Plant Nutr.* 2020; **43**, 2383-94.
[18] NL Fernando, DT Rathnayake, N Kottegoda, JS Jayanetti, V Karunaratne and DR Jayasundara. Mechanistic insights into interactions at urea-hydroxyapatite nanoparticle interface. *Langmuir* 2021; **37**, 6691-701.
[19] Z Lou, Q Zeng, X Chu, F Yang, D He, M Yang, M Xiang, X Zhang and H Fan. First-principles study of the adsorption of lysine on hydroxyapatite (100) surface. *Appl. Surf. Sci.* 2012; **258**, 4911-6.
[20] N Almora-Barrios, KF Austen and NHD Leeuw. Density functional theory study of the binding of glycine, proline, and hydroxyproline to the hydroxyapatite (0001) and (0110) surfaces. *Langmuir* 2009; **25**, 5018-25.
[21] R Astala and M Stott. First-principles study of hydroxyapatite surfaces and water adsorption. *Phys. Rev. B Condens. Matter.* 2008; **78**, 075427.
[22] N Kottegoda, N Madusanka and C Sandaruwan. Two new plant nutrient nanocomposites based on urea coated hydroxyapatite: Efficacy and plant uptake. *Indian J. Agr. Sci.* 2016; **86**, 494-9.
[23] MR Maghsoodi, N Najafi, A Reyhanitabar and S Oustan. Hydroxyapatite nanorods, hydrochar, biochar, and zeolite for controlled-release urea fertilizers. *Geoderma* 2020; **379**, 114644.
[24] S Pradhan, M Durgam and DR Mailapalli. Urea loaded hydroxyapatite nanocarrier for efficient delivery of plant nutrients in rice. *Arch. Agron. Soil Sci.* 2021; **67**, 371-82.
[25] P Bhavani, S Prakash, K Harinikumar, M Thimmegowda, P Benherlal and S Yoganand. Performance of slow release hydroxyapatite coated urea nanofertilizer on aerobic paddy. *Int. J. Curr. Microbiol. Appl. Sci.* 2020; **9**, 1320-30.
[26] HPG Reis, AS Giroto, GGF Guimarães, FF Putti, PS Pavinato, AP Teles, C Ribeiro and DM Fernandes. Role of slow-release phosphate nanofertilizers in forage nutrition and phosphorus lability. *ACS Agr. Sci. Tech.* 2022; **2**, 564-72.
[27] MJ Frisch, GW Trucks, HB Schlegel, GE Scuseria, MA Robb, JR Cheeseman, G Scalmani, V Barone, B Mennucci, GA Petersson, H Nakatsuji, M Caricato, X Li, HP Hratchian, AF Izmaylov, J Bloino, G Zheng, JL Sonnenberg, M Hada, M Ehara, ..., DJ Fox. *Gaussian ~09 revision D.01*. ScienceOpen, Inc., Berlin, Germany, 2014.
[28] J Tirado-Rives and W Jorgensen. Performance of B3LYP density functional methods for a large set of organic molecules. *J. Chem. Theor. Comput.* 2008; **4**, 297-306.
[29] JC Elliott, P Mackie and R Young. Monoclinic hydroxyapatite. *Science* 1973; **180**, 1055-7.
[30] V Bystrov, E Paramonova, Y Dekhtyar, A Katashev, A Karlov, N Polyaka, A Bystrova, A Patmalnieks and A Kholkin. Computational and experimental studies of size and shape related physical properties of hydroxyapatite nanoparticles. *J. Phys. Condens. Matter* 2011; **23**, 065302.
[31] R Tian, G Yang, Y Tang, X Liu, R Li, H Zhu and H Li. Origin of hofmeister effects for complex systems. *PLos One* 2015; **10**, e0128602.
[32] Q Wang, C Zhu, J Yun and G Yang. Isomorphic substitutions in clay materials and adsorption of metal ions onto external surfaces: A DFT investigation. *J. Phys. Chem. C* 2017; **121**, 26722-32.
[33] F Li and Z Chen. Tuning electronic and magnetic properties of MoO_3 sheets by cutting, hydrogenation, and external strain: A computational investigation. *Nanoscale* 2013; **5**, 5321-33.
[34] VS Bystrov. Computational studies of the hydroxyapatite nanostructures, peculiarities and properties. *Math. Biol. Bioinformatics* 2017; **12**, 14-54.

[35] IJ Bruno, JC Cole, PR Edgington, M Kessler, CF Macrae, P McCabe, J Pearson and R Taylor. New software for searching the cambridge structural database and visualizing crystal structures. *Acta Crystallogr. B* 2002; **58**, 389-97.
[36] I Streeter and NHD Leeuw. Binding of glycosaminoglycan saccharides to hydroxyapatite surfaces: A density functional theory study. *Proc. Roy. Soc. A Math. Phys. Eng. Sci.* 2011; **467**, 2084-101.
[37] T Lu and F Chen. Multiwfn: A multifunctional wavefunction analyzer. *J. Comput. Chem.* 2012; **33**, 580-92.
[38] ER Johnson, S Keinan, P Mori-Sánchez, J Contreras-García, AJ Cohen and W Yang. Revealing noncovalent interactions. *J. Am. Chem. Soc.* 2010; **132**, 6498-506.
[39] A Mubarik, N Rasool, MA Hashmi, A Mansha, M Zubair, MR Shaik, MA Sharaf, EM Awwad and A Abdelgawad. Computational study of structural, molecular orbitals, optical and thermodynamic parameters of thiophene sulfonamide derivatives. *Crystals* 2021; **11**, 211.
[40] C Karnan, K Nagaraja, S Manivannan, A Manikandan and V Ragavendran. Crystal structure, spectral investigations, DFT and antimicrobial activity of brucinium benzilate (BBA). *J. Mol. Model.* 2021; **27**, 1-11.
[41] MH Kebiroglu, C Orek, N Bulut, O Kaygili, S Keser and T Ates. Temperature dependent structural and vibrational properties of hydroxyapatite: A theoretical and experimental study. *Ceram. Int.* 2017; **43**, 15899-904.
[42] NMN Najwa-Alyani and LS Ang. Selecting suitable functionals and basis sets on the study structural and adsorption of urea-kaolinite system using cluster method. *Indonesian J. Chem.* 2022; **22**, 361-73.